

Dynamic Response of an Inverted flag Subjected to a Cylinder Wake

S. Izawa^{1*}, S. Saito¹ and A. Kase¹

¹: Faculty of Engineering, University of Toyama, Japan

* Correspondent author: sizawa@eng.u-toyama.ac.jp

Abstract

The effect of an upstream circular cylinder on the dynamics of a downstream inverted flag is investigated using a two-dimensional incompressible SPH method together with fluid-structure interaction model. When the flag is placed just behind the cylinder, periodic vortex shedding is suppressed, and a quasi-straight state is only observed. As the separation distance increases, the flag still remains stationary though the vortex shedding takes place at the same frequency as that of the isolated flag. The flag further away from the cylinder exhibits a different behavior depending on the original vibration modes without the cylinder. While the flags in the straight and flapping modes are free of the influence of the cylinder wake, the flag in the bending mode is flapping in synchronization with oncoming shedding vortices. Its oscillation frequency thus equals to an integral submultiple of the vortex shedding frequency of the upstream cylinder, not to the natural frequency.

Keyword: *Inverted flag, Wake, Flow-induced vibration, SPH*

1. Introduction

The flow-induced vibration of flexible bodies can be found not only in our daily lives but also in many engineering applications, e.g., paper flutter in the printing process, airfoil/vane flutter, and long-span suspension bridges. In recent years, much focus has been placed on their energy harvesting applications in which the elastic strain energy due to solid deformation is converted into the electric current via piezoelectric materials. Among them, flag flapping is a promising candidate for energy harvesting devices; however, a conventional flag configuration with a clamped leading edge and a free trailing edge cannot provide sufficient power generation in a low-velocity environment. Kim et al. [1] have examined an alternative configuration, i.e., an inverted flag, in which the leading edge is free to move and the trailing edge is clamped, demonstrating that it can flap with a large amplitude even in breezy conditions.

Onset of flapping is generally due to a divergence instability, or a static bifurcation of the zero-deflection equilibrium state. As the flow speed increases and exceeds a certain threshold, the inverted flag of infinite aspect ratio becomes unstable and starts to deflect outward. Sader et al. [2] pointed out that flapping is a vortex-induced vibration occurring subsequent to the divergence instability. In other words, unsteady force acting on the flag is a key to a large amplitude oscillation, except for heavy flags. Hu et al. [3] found that the leading-edge serrations can significantly improve the flapping amplitude by delaying the flow separation. Various configurations have also been tested for inverted flags to induce large oscillations with the help of hydraulic coupling of multiple objects. For instance, Zou et al. [4] numerically studied the side-by-side configuration of two flags, and the three flag configurations in which one more flag is added in front or rear of the side-by-side flags. The wake of bluff body is also used to destabilize a downstream flag. Kim et al. [5] experimentally studied the effect of an upstream flat plate on a downstream flag, either inverted flag or conventional flag. Umair et al [6] reported the impact of a bluff body on the energy harvesting performance of an inverted piezoelectric flag at different bending stiffness.

In this study, we numerically investigate the dynamic response of an inverted flag in the wake of a circular cylinder by focusing on the vortex interaction with the flag. Two-dimensional simulations are performed using an incompressible smoothed particle hydrodynamics (SPH) method together with a fluid-structure interaction model proposed by Nishiura et al. [7].

2. Numerical Method and Problem Setting

2.1 Fluid simulation

SPH is a Lagrangian method in which the continuum is discretized into finite particles interacting with each other, and then the flow is directly calculated by their movements. In SPH, an arbitrary function is given in the integral form by using an interpolation function, named the kernel function, and its spatial derivative is obtained simply by differentiating the kernel function. Since particle migration results in a local variation in density, special treatment is required for satisfying the incompressible condition, i.e., density homogeneity. The present study enforces the incompressibility by adjusting the disordered particle locations at each time step after fluid particles move according to their inertia in analogy with a predictor-modifier method. By repeating this process N times, the density at each particle gradually approaches a constant value [7]. For a given particle i , the velocity is updated as follows,

$$\mathbf{v}_i(t + \Delta t) = (\mathbf{v}_i(t) + \mathbf{f}_i \Delta t) + \sum_k^N \Delta \mathbf{v}_{i,\text{corr}}^{(k)}$$

where \mathbf{f} is the force per unit mass acting on the fluid particles except for the pressure gradient force, the first term on the RHS is the first velocity predictor, and $\Delta \mathbf{v}_{i,\text{corr}}^{(k)}$ is the k -th velocity corrector given by

$$\Delta \mathbf{v}_{i,\text{corr}}^{(k)} = -c^2 \sum_j m_j \left(\frac{\tilde{\rho}_i^{(k)} - \rho_0}{\tilde{\rho}_i^{(k)2}} + \frac{\tilde{\rho}_j^{(k)} - \rho_0}{\tilde{\rho}_j^{(k)2}} \right) \nabla_i W_{ij}$$

where c is the speed of sound, m is the mass of fluid particle, ρ_0 is the reference density of the fluid, and $\tilde{\rho}^{(k)}$ is the density at the tentative particle location. The number of iterations is set to 5 because larger N will increase the numerical viscosity. It is noted that during the process, flag particles are treated as stationary fluid particles.

2.2 Fluid-structure interaction

A flag consists of a single layer of particles aligned in a line with constraints between the particles. The forces due to the elasticity and the bending stiffness are modeled by the particle-based membrane model [7]. The equations of motion of the flag are given by

$$m_s \frac{d^2 \mathbf{r}_i}{dt^2} = \mathbf{T}_i + \mathbf{B}_i + \mathbf{F}_i$$

where m_s is the mass of flag particle, \mathbf{T}_i is the stretching force between two adjacent particles, \mathbf{B}_i is the force derived from the bending moment, and \mathbf{F}_i is the fluid force acting on each flag particle estimated by integrating the reaction forces from the fluid particles located next to the flag particle during the density homogenization process. The time step of the structure movement is empirically set to one-thousandth of the time step of the fluid motion because the numerical integration become unstable when a larger time incrementation is used. During the 1,000 time steps for structure computation, the same fluid force \mathbf{F}_i is used.

2.3 Problem setting

The computational domain is shown in Fig. 1. A circular cylinder with a diameter of $D (= 11h)$ is placed $60h$ away from the inlet boundary, and a flag with a length of $L (= 31h)$ and a thickness of h is placed

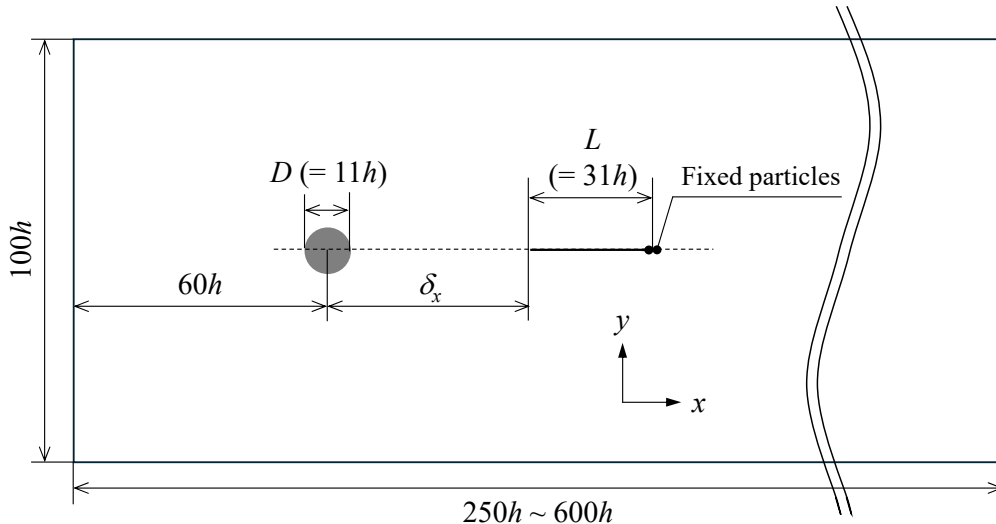


Figure 1 Computational domain/

Dynamic Response of an Inverted flag Subjected to a Cylinder Wake

downstream, δ_x , away from the cylinder. Here, h is the smoothing length of the kernel. Two downstream flag particles are fixed, constituting the support. While the y -domain is constant at $100h$, the x -domain is changed from $250h$ to $600h$, depending on the distance δ_x . A uniform velocity U is given at the inlet boundary, and the Neumann condition is given at the outlet boundary where the adjustments are made so that the averaged velocity of the leaving particles is equal to U . Periodic boundary conditions are used in the y direction. The flag is initially disturbed in the y direction to reduce the computational cost.

The flapping motion of a flag (Young's modulus E and Poisson's ratio σ) is characterized by following three nondimensional numbers,

$$Re = \frac{\rho UL}{\mu}, \quad B^* = \frac{B}{\rho U^2 L^3}, \quad M^* = \frac{\rho_s h}{\rho L}$$

where ρ is the fluid density, μ is the viscosity, B is the bending stiffness of the sheet ($B = Eh^3/12(1 - \sigma^2)$), and its density ρ_s . Among these system parameters, the Reynolds number and the mass ratio are fixed at $Re = 496$ and $M^* = 0.147$, respectively. The bending stiffness B^* is chosen from the vibration mode from an isolated inverted flag without a cylinder.

3. Results and Discussion

3.1 Inverted flag in a uniform flow

First, the amplitude and flapping frequency of the elastic flag in a uniform flow are examined while changing the bending rigidity. The results are shown in Fig. 2, where A and f represent the peak-to-peak amplitude and the frequency. The large-amplitude flapping crossing the mid plane occurs at nondimensional bending stiffness B^* in the range of 1.72×10^{-3} to 4.06×10^{-3} . Within this regime, the Strouhal number fA/U increases in proportion to B^* . This flapping mode is characterized by a plateau at $A/L > 1.6$ and a gradual increase in fA/U , in agreement with the experimental study by Kim et al. (2013) [1]. When the restoring force is superior to the destabilizing fluid force ($B^* > 4.06 \times 10^{-3}$), the initial disturbance decays exponentially in time and the flag eventually approaches to a straight state (straight mode). Also, when B^* falls below 1.72×10^{-3} , the flag just bends on the initially disturbed side without flapping (deflected mode). A further decrease in B^* gives way to the deflected flapping mode at which the flag rolls backward past a maximum $|y|$ position and only the near tip region is flapping (deflected-flapping mode). In the next sections, we will then discuss the effect of the unsteady wake on the downstream flag motion at each mode: 4.52×10^{-3} (straight mode), 2.71×10^{-3} (flapping mode), and 1.36×10^{-3} (deflected mode).

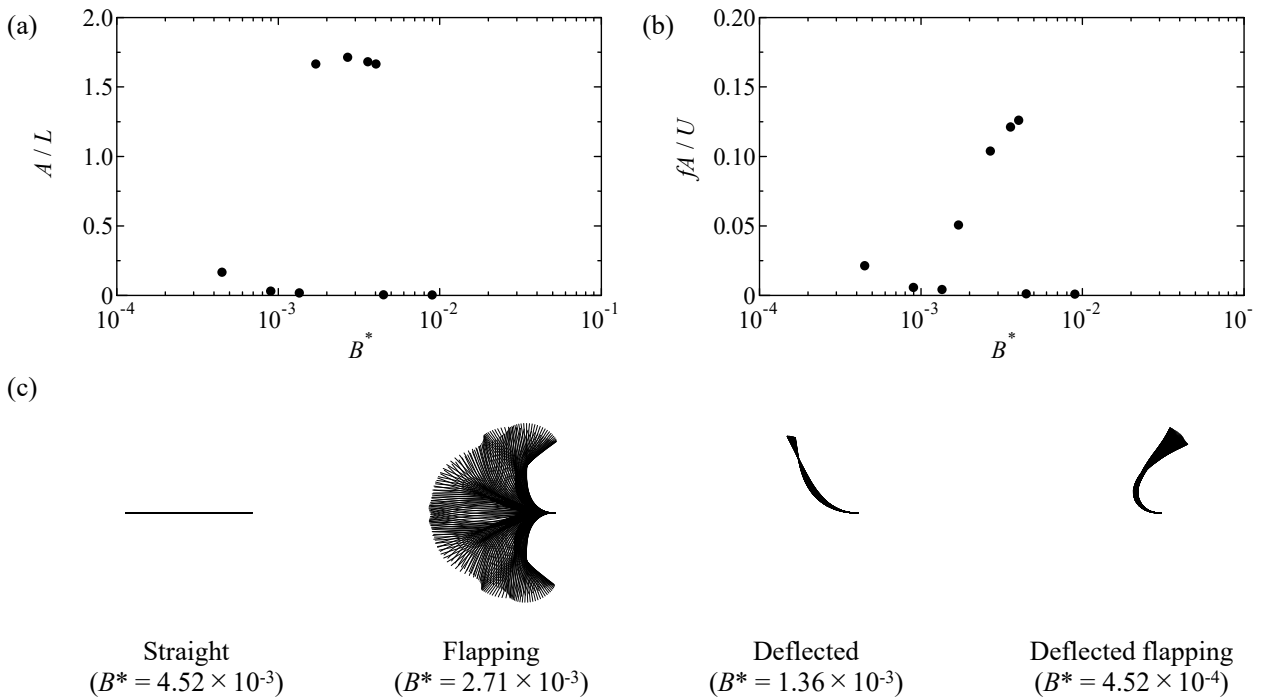


Figure 2 (a) Peak-to-peak amplitude A/L of the tip, (b) Strouhal number fA/U , and (c) superimposed images of the flag at different bending stiffness values (without cylinder).

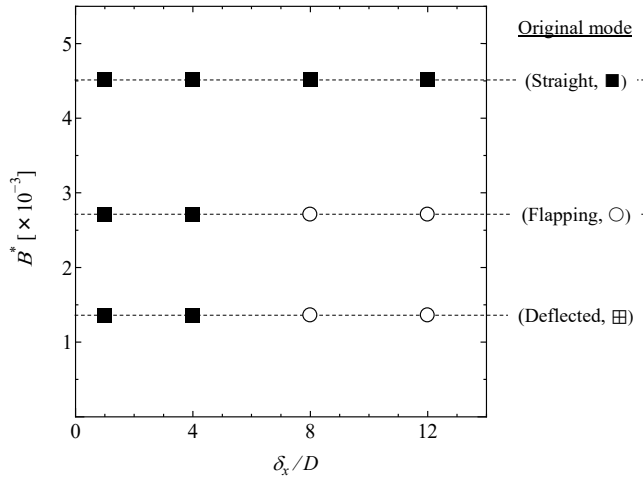


Figure 3 Mode transition diagram for each B^* : 4.52×10^{-3} (straight mode, ■), 2.71×10^{-3} (flapping mode, ○) and 1.36×10^{-3} (deflected mode, □). The wake-induced vibration modes are plotted in the figure.

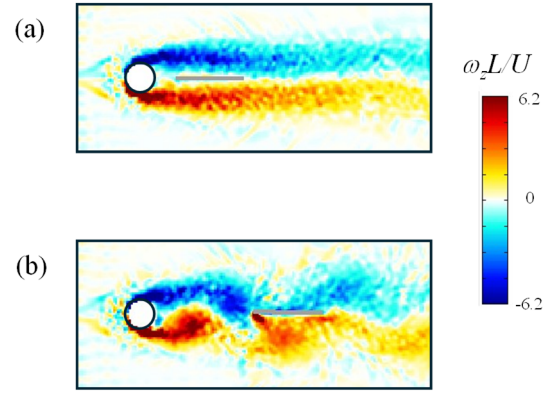


Figure 4 Instantaneous vorticity contours for the inverted flag of $B^* = 4.52 \times 10^{-3}$ at $\delta_x/D = 1.0$ (a) and 4.0.

3.2 Inverted flag in a cylinder wake

The Reynolds number based on the diameter of the cylinder D is set to 176 at which periodic vortex shedding takes place at 0.012 Hz. The relative size of the cylinder to the peak-to-peak amplitude of the isolated inverted flag in the flapping mode D/A is approximately 0.22. The mode transition diagram for the flag subjected to the unsteady wake of the cylinder is summarized in Fig. 3. The resulting vibration mode depends on the distance between the flag and the cylinder. When the flag is very close to the cylinder ($\delta_x/D < 4$), it exhibits the straight mode without any vibration regardless of the bending stiffness. Besides, the periodic vortex shedding is suppressed by interrupting the interaction between the upper and lower free shear layers, as shown in Fig. 4a. At $\delta_x/D = 4$, the vortex shedding takes place at the same frequency as that of the isolated flag (see Fig. 4b).

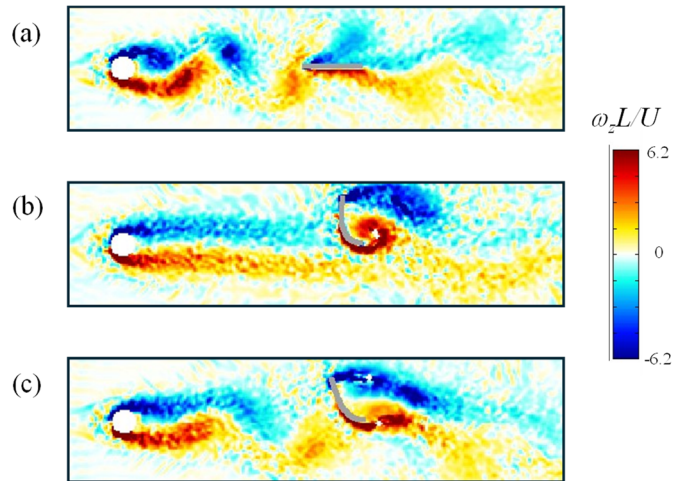


Figure 5 Instantaneous vorticity contours for the inverted flag of $B^* = 4.52 \times 10^{-3}$ (a), 2.71×10^{-3} (b) and 1.36×10^{-3} (c) at $\delta_x/D = 8.0$.

However, the flag still remains a quasi-stationary state though it is shaken every time the shedding vortices pass by. The flag further away from the cylinder exhibits a different behavior depending on the original vibration modes without the cylinder. The flags in the straight mode and the flapping mode are free of the influence of the cylinder wake; the flapping frequency is exactly the same as that without the cylinder (Fig. 5a and 5b). On the other hand, large-amplitude flapping is observed for the flag in the bending mode. Spectral analysis reveals that the vibration frequencies at $\delta_x/D = 8$ and 12 equal to 1/18 and 1/15 of the vortex shedding frequency of the upstream cylinder 0.010 ~ 0.012 Hz, not to the natural frequency of the flag, 0.0032 Hz. This fact indicates that the flag in the bending mode is flapping in synchronization with oncoming shedding vortices.

Figure 6 plots the spatial variation of the magnitude of the fluid force acting on the flag in the bending mode at different time steps when the flag is bending downward. Here, the ξ coordinate denotes the distance from the leading edge along the flag surface. The negative and positive vortices released from the cylinder collide with the flag at around $Ut/D = 140.7$ and 149.4, respectively. The flag receives strong force at these timings,

Dynamic Response of an Inverted flag Subjected to a Cylinder Wake

especially for the near-tip region. The temporal variation of the magnitude of the tip velocity $|\bar{v}|$ is shown in Fig. 7, where a lowpass filter with cutoff frequency of 20 Hz is used to eliminate the noise. The flag is strongly accelerated in the bending direction at around $Ut/D = 135 \sim 140$ and $145 \sim 150$. These findings suggest that the flag is flapping in synchronization with an oncoming vortex street.

4. Conclusions

The response of an inverted flag to the wake of a circular cylinder was numerically studied using an incompressible SPH method and a fluid-structure interaction model. When the distance between the cylinder and the flag is very small, the flag is trapped in the cylinder wake keeping the straight mode irrespective of the bending stiffness. As the distance increases, the periodic vortices are shed from the cylinder at the same frequency as that of the isolated flag; however, the flag still remains stationary. At higher separation distance, the flag exhibits a different behavior depending on the original vibration modes without the cylinder. The wake effect is negligible for the flags in the straight and flapping modes. They main the same mode. On the other hand, large amplitude vibration occurs for the flag in the bending mode in synchronization with oncoming shedding vortices.

References (Example)

- [1] Kim, D., Cossé, J., Cerderia, H. and Gharib, M., “Flapping dynamics of an inverted flag”, *Journal of Fluid Mechanics*, Vol. 736, R1, (2013).
- [2] Sader, J. E., Cossé, J., Kim, D., Fan, B. and Gharib, M., “Large-amplitude flapping of an inverted flag in a uniform steady flow – a vortex-induced vibration”, *Journal Fluid Mechanics*, Vol. 793, (2016). pp. 524-555.
- [3] Hu, YW., Feng, LH. and Wang, JJ., “Effect of leading-edge serration on the flow-structure interactions of an inverted flag”, *Experiments in Fluids*, Vol. 63, No. 133, (2022).
- [4] Zou, K., Peng, ZR. Chen, B., Dai, H., Xiong, Y. and Wang, L., “Hydrodynamic coupling of inverted flags in side-by-side, left triangular and right triangular configurations in a uniform flow”, *Frontiers in Physics*, Vol. 10, (2022).
- [5] Kim, H., Kang, S. and Kim, D., “Dynamics of a flag behind a bluff body”, *Journal of Fluid Science and Structures*, Vol. 71 (2017), pp. 1-14.
- [6] Umair, M., Latif, U., Uddin, E. and Abdelkefi, A., “Experimental hydrodynamic investigations on the effectiveness of inverted flag-based piezoelectric energy harvester in the wake of bluff body”, *Ocean Engineering*, Vol. 245, 110454, (2022).
- [7] Nishiura, K., Nishio, Y., Izawa, S. and Fukunishi, Y., “Flapping motion of a permeable flag in uniform flow”, *Fluid Dynamics Research*, Vol. 51, 025506, (2019).
- [8] Fukunishi, Y., Takahashi, Y., Nishio, Y. and Izawa, S., “Attempt to suppress numerical viscosity in incompressible SPH method”, *Journal of Applied Fluid Mechanics*, Vol. 12, No. 4, (2018), pp. 1231-1240.

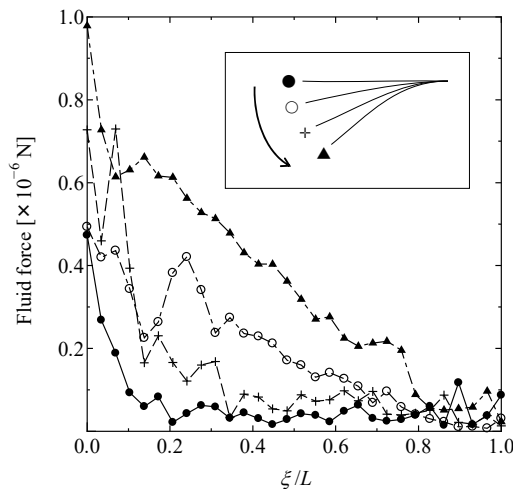


Figure 6 Spatial variation of the fluid force acting on the flag ($B^* = 1.36 \times 10^{-3}$) at $Ut/D = 136.4$ (●), 140.7 (○), 145.6 (+) and 149.4 (▲).

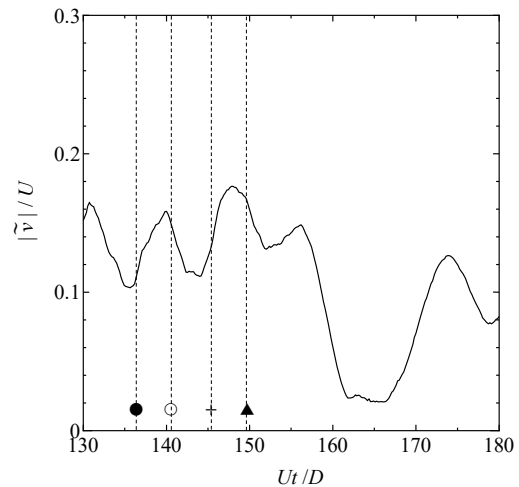


Figure 7 Temporal variation of the lowpass -filtered tip velocity ($B^* = 1.36 \times 10^{-3}$).